Revealing Hofstadter Spectrum for Graphene in a Periodic Potential

Godfrey Gumbs[1,2], Andrii Iurov[1] *, Danhong Huang[3] and Liubov Zhemchuzhna[4]
[1]*Department of Physics and Astronomy, Hunter College of the City University of New York, 695 Park Avenue, New York, NY 10065, USA*
[2] *Donostia International Physics Center (DIPC), P de Manuel Lardizabal, 4, 20018 San Sebastian, Basque Country, Spain*
[3]*Air Force Research Laboratory, Space Vehicles Directorate Kirtland Air Force Base, NM 87117, USA*
[4]*Department of Math & Physics, North Carolina Central University, Durham, North Carolina 27707, USA*
(Dated: March 27, 2014)

We calculate the energy bands for graphene monolayers when electrons move through a periodic electrostatic potential in the presence of a uniform perpendicular magnetic field. We clearly demonstrate the quantum fractal nature of the energy bands at reasonably low magnetic fields. We present results for the energy bands as functions of both wave number and magnetic flux through the unit cells of the resulting moiré superlattice. The effects due to pseudo-spin coupling and Landau orbit mixing by a strong scattering potential have been exhibited. At low magnetic fields when the Landau orbits are much larger than the period of the modulation, the Landau levels are only slightly broadened. This feature is also observed at extremely high magnetic fields. The density of states has been calculated and shows a remarkable self-similarity like the energy bands. We estimate that for modulation period of $10\,nm$ the region where the Hofstadter butterfly is revealed at $B \leq 2\,T$.

PACS numbers: 73.22-f, 73.22 Pr., 71.15.Dx, 71.70.Di, 81.05.U-
Keywords: Hofstadter butterfly, fractal structures, Landau levels, graphene

arXiv:1403.6534v1 [cond-mat.mes-hall] 25 Mar 2014

In recent experiments [1–3], graphene flake and bilayer graphene were coupled to a rotationally-aligned hexagonal boron nitride substrate. The spatially varying interlayer electrostatic potential gives rise to local symmetry breaking of the carbon sublattice as well as a long-range moiré superlattice potential in the graphene layer. At high magnetic fields, integer conductance plateaus which were obtained at non-integer filling factors were believed to be due to the formation of the Hofstadter butterfly in a symmetry-broken Landau level. These experiments were partially motivated by the pioneering theoretical work of Azbel [4] and Hofstadter [5] on the single-particle spectrum of a two-dimensional structure in the presence of both a periodic potential and a uniform ambient perpendicular magnetic field. In this case, the energies exhibit a self-similar recursive energy spectrum. There are several other effects due to the presence of boron nitride substrate. The band gaps, which appear in graphene due to the substrate, were theoretically modeled in [6]. The existence of a commensurate state, when the crystal is adjusted by the presence of the external periodic potential, has been investigated in [7]. Hofstadter fractal structures may also be realized in a variety of systems, such as Jaynes-Cummings-Hubbard lattices [9]. We should also mention a recent study of the energy spectrum of Schrödinger electrons, subjected to general periodic potential and magnetic field [8].

The fractal nature of the Hofstadter butterfly had captivated researchers for many years [10–26]. The paper by Hofstadter [5] was for the energy spectrum of a periodic square lattice in the tight-binding approximation and subject to a perpendicular magnetic field. Ever since that time, there have been complementary calculations for the hexagonal lattice [10], the two-dimensional electron gas (2DEG) with an electrostatic periodic modulation potential [17, 18, 26] and even bilayer graphene where different stacking of the two types of atoms forming the sublattices was considered [27]. It has been claimed that one may be able to observe evidence of the existence of Hofstadter's butterfly in such experimentally measured quantities as density-of-states and conductivity of the 2DEG [2, 3, 29].

The challenge facing experimentalists had been to carry out experiments on 2D structures at achievable magnetic fields where the Hofstadter butterfly spectrum is predicted. However, both monolayer and bilayer graphene coupled to hexagonal boron nitride provide a nearly ideal-sized periodic modulation, enabling unprecedented experimental access to the fractal spectrum [1–3].

In formulating a theoretical framework for the energy band structure for a periodically modulated energy band structure in a uniform magnetic field, one may adopt the procedure of Hofstadter by using Harper's equation which may be viewed as a tight-binding approximation of the Schrödinger equation.Additionally, assuming that the magnetic flux through unit cell of the periodic lattice is a rational fraction p/q of the flux quantum in conjunction with the Bloch condition for the wave function, one obtains a $p \times p$ Hamiltonian matrix to determine the energy eigenvalues since

* E-mail: theorist.physics@gmail.com

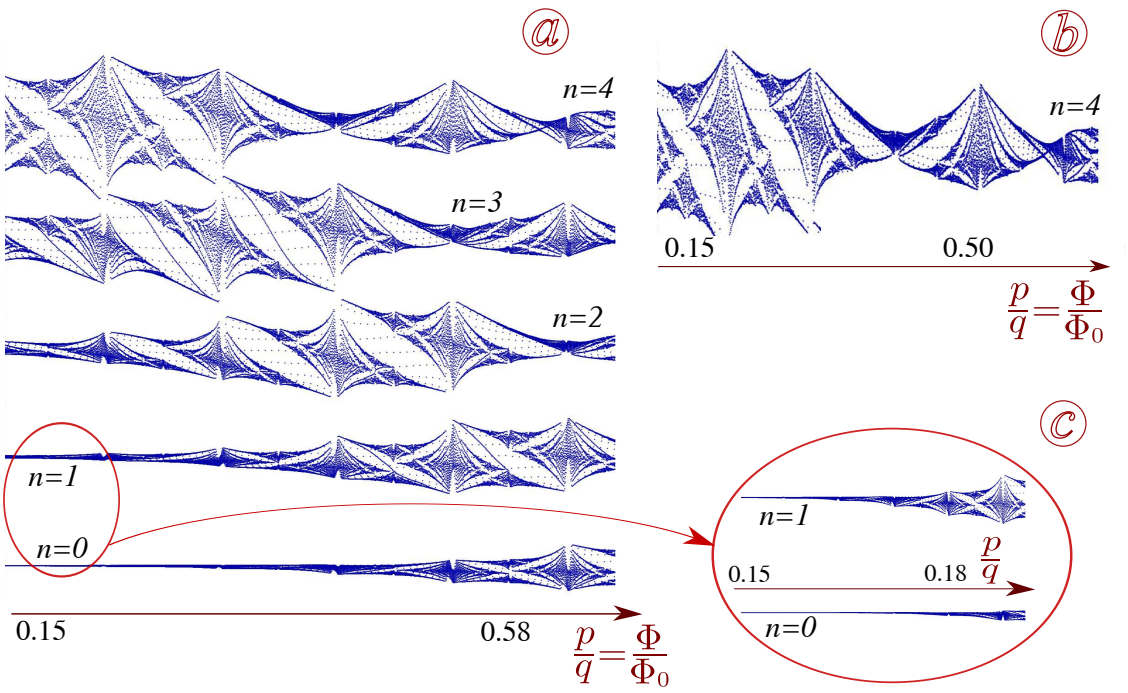

FIG. 1: (Color online) Energy band structure of a weakly modulated 2DEG as a function of magnetic flux ratio p/q. Plot (a) presents the four lowest Landau subbands for chosen modulation strength $\mathbb{V}_0 = 0.5\,\hbar\omega_c$, $N = 10$ and $k_x = k_y = 0.3$ in units of $2\pi/d_x$. Plot (b) shows the detailed band structure of the $n = 4$ Landau level for a 2DEG. Panel (c) shows a zoom-in of the low-field portion of the two lowest levels for a 2DEG, demonstrating self-repeated structures for all levels and magnetic field.

one only needs to solve the problem in a unit cell. Hofstadter himself was concerned about ever reaching magnetic fields where the rich self-similar structure of the butterfly would be experimentally observed due to the estimated high fields required to achieve this.

In this paper, we supplement the recent experimental work on graphene by first presenting a formalism for calculating the energy band structure when an electrostatic modulation potential is applied to a flat sheet in the presence of a reasonably low perpendicular magnetic field. These results are then employed in a calculation of the density-of-states (DoS). Our results may be verified experimentally since the DoS is directly proportional to the quantum capacitance [28]. The DoS may also be obtained from magnetic susceptibility measurements. For a review of related energy band structure studies, see [25]. We also compare our results with those for a modulated two-dimensional electron gas and discuss the difference.

In the presence of a uniform perpendicular magnetic field B_0 and periodic two-dimensional electrostatic *modulation potential* defined by [26]

$$\mathbb{V}(x,\,y) = \mathbb{V}_0 \left[\cos\left(\frac{\pi x}{d_x}\right)\cos\left(\frac{\pi y}{d_y}\right)\right]^{2N}\,, \tag{1}$$

where $N = 1,\,2,\,\cdots$ is an integer determining the size of the scatterers, the parameter $\mathbb{V}_0$ is the modulation amplitude, and d_x, d_y are the modulation periods in the x and y directions, respectively, we rewrite the Hamiltonian operator as

$$\mathcal{H} = \begin{bmatrix} \mathbb{V}(x,y) & \hat{p}_x + eB_0 y\hat{x}_0 + \imath\hat{p}_y \\ \hat{p}_x + eB_0 y\hat{x}_0 - \imath\hat{p}_y & \mathbb{V}(x,y) \end{bmatrix} \tag{2}$$

For this new system, the magnetic flux per unit cell is $\Phi = B_0(d_x d_y)$, which is assumed to be a rational fraction of the flux quantum $\Phi_0 = \hbar/e$, i.e., $\beta \equiv \Phi/\Phi_0 = p/q$, where p and q are prime integers. Furthermore, we choose the first Brillouin zone defined by $|k_x| \le \pi/d_x$ and $|k_y| \le \pi/(qd_y)$.

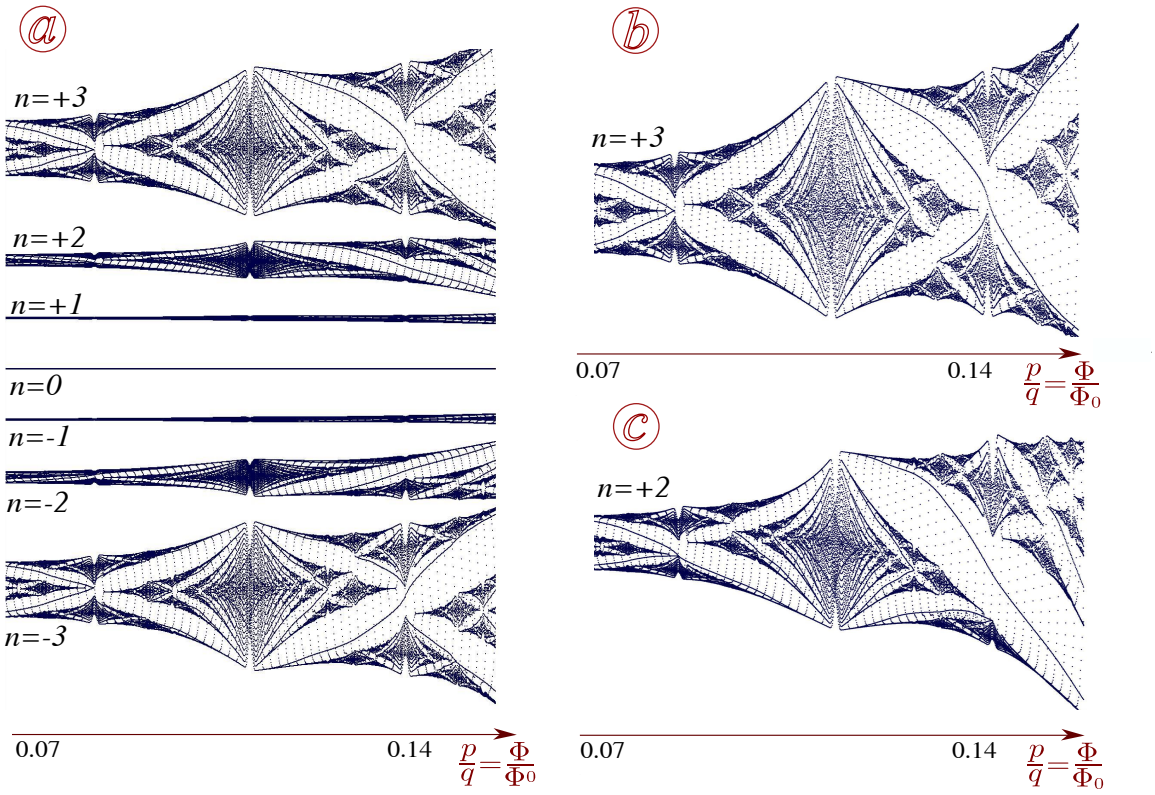

FIG. 2: (Color online) Band structure of strongly modulated graphene as a function of magnetic flux ratio p/q. Plot (a) gives the lowest few Landau subbands from both valence and conduction bands for a chosen modulation $\mathbb{V}_0 = 2.0\,\hbar\omega_c$ and $k_x = k_y = 0.3/d_x$. Plots (b) and (c) show details of the band structure of the $n = +2$ and $n = +3$ Landau levels. The levels are not mixed.

By using the Bloch-Peierls condition, the wave function of this system may be expanded as

$$\Phi^{\pm}_{\ell;\,n,\vec{k}_{||}}\,(x,\,y) = \frac{1}{\sqrt{2\mathcal{N}_y}} \sum_{s=-\infty}^{\infty} \mathrm{e}^{ik_y\ell_B^2(sp+\ell)K_1}\,\Psi^{K,\pm}_{n,k_x-(sp+\ell)K_1}\,(x,\,y) \tag{3}$$

where $\vec{k}_{||} = (k_x,\,k_y)$, $\mathcal{N}_y = L_y/(qd_y)$ is the number of unit cells, which are spanned by $b_1 = (d_x,\,0)$ and $b_2 = (0,\,qd_y)$, in the y direction, L_y $(\to \infty)$ is the sample length in the y direction, $K_1 = 2\pi/d_x$ is the reciprocal lattice vector in the x direction and $\ell = 1,\,2,\,\cdots,\,p$ is a new quantum number for labeling split p subbands from a k_x-degenerated landau level in the absence of modulation. The above wave function satisfies the usual Bloch condition:

$$\Phi^{\pm}_{\ell;\,n,\vec{k}_{||}}\,(x+d_x,\,y+qd_y) = \mathrm{e}^{ik_xd_x}\,\mathrm{e}^{ik_yqd_y}\,\Phi^{\pm}_{\ell;\,n,k_{||}}\,(x,\,y)\ . \tag{4}$$

Since the wave functions at K and K' points are decoupled from each other for monolayer graphene, which is different from bilayer graphene, [30] we can write out explicitly the full expression for the wave function at these two points. A tedious but straightforward calculation yields the magnetic band structure for this modulated system as a solution of the eigenvector problem $\mathcal{M}\bigotimes\vec{\mathcal{A}}(\vec{k}_{||}) = 0$ with the coefficient matrix $\overleftrightarrow{\mathcal{M}}$ given by

$$\{\mathcal{M}\}_{j,\,j'} = \left[E^{\mu}_n - \varepsilon(\vec{k}_{||})\right]\delta_{n,n'}\delta_{\ell,\ell'}\delta^{(n)}_{\mu,\mu'} + \ \mathbb{V}^{\ell',n',\mu'}_{\ell,n,\mu}(\vec{k}_{||})\ , \tag{5}$$

where $\delta^{(n)}_{\mu,\mu'} = 1$ for $n = 0$ and $\delta^{(n)}_{\mu,\mu'} = \delta_{\mu,\mu'}$ for $n > 0$, $j = \{n,\,\ell,\,\mu\}$ is the composite index, and $\{\vec{\mathcal{A}}(\vec{k}_{||})\}_j = \mathcal{A}^{\mu}_{n,\ell}(\vec{k}_{||})$ is the eigenvector. The eigenvalue $\varepsilon_\nu(\vec{k}_{||})$ of the system is determined by $\mathrm{Det}\{\overleftrightarrow{\mathcal{M}}\} = 0$. Here we calculate $\mathbb{V}^{\ell',n',\mu'}_{\ell,n,\mu}(\vec{k}_{||})$ as the Fourier transform. The detailed derivation of these matrix elements could be found in [31].

Fig. 1 shows that for a 2DEG, the lowest perturbed Landau subband which originates from the unperturbed $n = 0$ Landau level merges with the resulting butterfly spectrum at the highest magnetic field compared to the

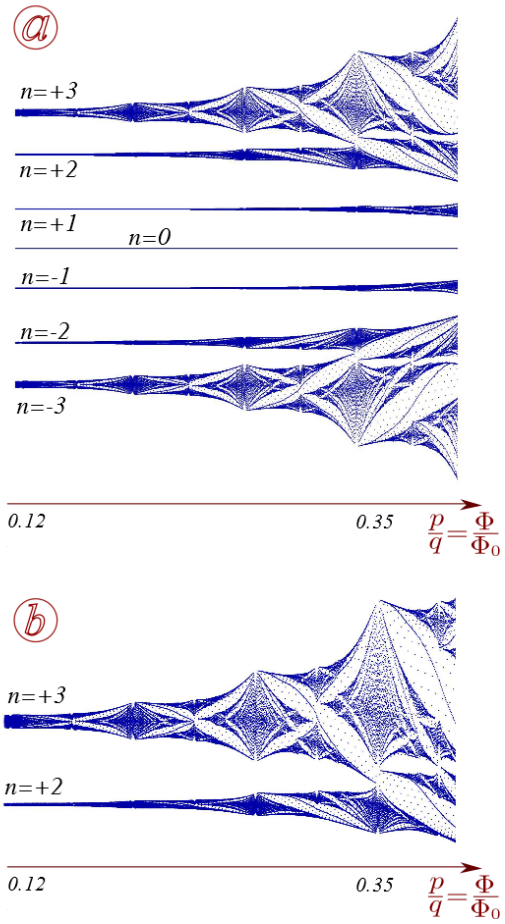

FIG. 3: (Color online) (Color online) Band structure of a modulated graphene monolayer as a function of magnetic (flux ratio p/q). Plot (a) demonstrates the lowest few Landau subbands from both valnece and conduction bands for a chosen modulation $\mathbb{V}_0 = 5.0\,\hbar\omega_c$ and $k_x = k_y = 0.3$. Plot (b) and (c) show the structure of $(n = +2)$ and $(n = +3)$ Landau level. The levels are mixed.

$n = 1, 2, 3, 4$ Landau levels in the conduction band. The onset of the butterfly takes place around $p/q = 1/5$ which would correspond to a magnetic field $B \approx 2$ T for $d_x = d_y = 10$ nm. Furthermore, our calculations have shown that for graphene the symmetry between the valence and conduction bands is destroyed by modulation. There is always mixing of the subbands regardless of the value for $\mathbb{V}_0$. This is in contrast with modulated 2DEG where for weak $\mathbb{V}_0$, the Landau subbands do not overlap as shown in Fig. 2. The lowest subband is shifted upward like the other subbands but is not widened as much as the higher subbands. The feature of self-similarity is also apparent in the excited subbands at intermediate magnetic fields. There is only a shift and broadening of the subbands in the low and high magnetic field regimes for modulated 2DEG.

The results of our calculations for the energy eigenvalues of modulated graphene as a function of magnetic flux appear in Fig. 2. We included the $n = 0, \pm1, \pm2, \pm3, \pm4$ as we did in obtaining Fig. 1. For weak magnetic fields, the Landau levels in both valence and conduction bands are slightly broadened into narrow subbands but shifted upward by the perturbing potential $\mathbb{V}_0$. Another effect due to modulation is to cause these Landau bands to have negative slope at weak magnetic fields which then broaden enough at higher magnetic fields to produce Landau orbit mixing, reflecting the commensurability the magnetic and lattice Brillouin zones. In Fig. 3, we demonstrate a Hofstadter dispersion plot for the case when at least two Landau levels are mixed, featuring a larger fractal self-repeated structure, which incorporates more than one energy level.

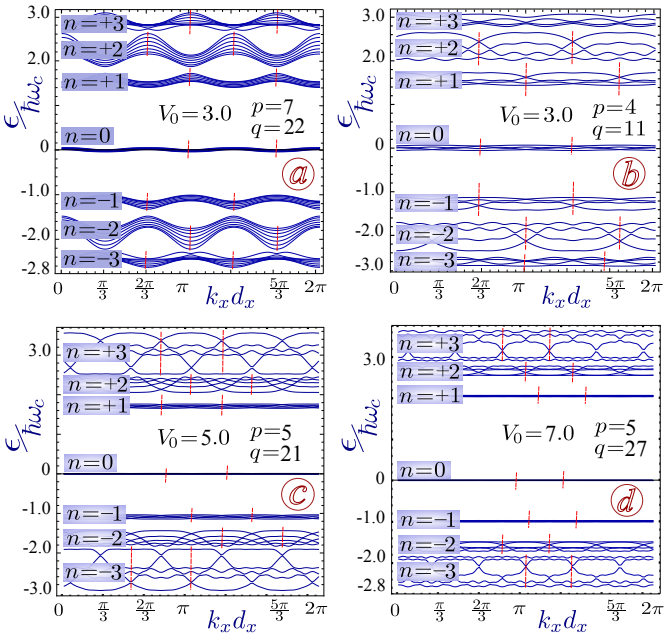

FIG. 4: (Color online) Energy dispersion as functions of $k_x d_x$ for graphene and 2DEG with chosen values of modulation potential $\mathbb{V}_0$ and magnetic flux p/q in units of the flux quantum. The energy is scaled in terms of $v_F\sqrt{Be\hbar}$.

In Fig. 4, we present the dispersion curves as a function of $k_x d_x$ for chosen value of $\mathbb{V}_0$ and two pairs of values of p and q corresponding to two different magnetic field strengths. In each case, there are p Landau subbands, q/p determines the number of oscillation periods in the first Brillouin zone for each of these subbands. Both the valence and conduction subbands are shifted upward but the conduction subbands are shifted more than the valence subbands for each corresponding Landau label for the unmodulated structure. This shift is increased when the modulation amplitude is increased. The original zero-energy Landau level is only slightly broadened and is the least affected by $\mathbb{V}_0$. If the sign of the modulation amplitude is reversed to correspond to an array of quantum dots, then the subbands are all shifted downward. from their positions for an unmodulated monolayer graphene.

We also calculate and display the density-of-states plots, which demonstrate the general magnetic field dependence of the Hofstadter spectrum, showing the general fractal structures independent of the specific values of the wave vector $\vec{k}_{\|}$. Based on the calculated eigenenergy $\varepsilon_\nu(\vec{k}_{||})$, we can further calculate the electron density of states in this system, given by

$$\rho(\varepsilon,\, B_0) = \frac{1}{2\pi^2 q d_x d_y} \sum_\nu \int_{-\pi/d_x}^{\pi/d_x} dk_x \int_{-\pi/(qd_y)}^{\pi/(qd_y)} dk_y \, \frac{\Gamma/\pi}{[\varepsilon - \varepsilon_\nu(\vec{k}_{||})]^2 + \Gamma^2} \;, \tag{6}$$

where Γ represents the level broadening.

Making use of our calculated energy eigenvalues $\epsilon_\nu(\vec{k})$, we further determine the electron density-of-states for monolayer graphene in the presence of a uniform perpendicular magnetic field.

A plot of the density-of-states as a function of magnetic field basically reproduces the Hofstadter self-repeating fractal structure, averaged over all allowed values of $\vec{k}$. In our calculations, the delta function is chosen as a Lorentzian. This leads to the finite width for the density of states for various values of energy ϵ. In this regard, one should look at Ref. [32], in which the density-of-states has been calculated for carbon nanotubes for the various cases of magnetic field strength and orientation.

Fig. 5 shows $\rho(\epsilon, B)\, B$. We chose this specific set of results obtained for the density-of-states to demonstrate the effect due to the modulation in order to show how the Hofstadter structure may be suppressed by the strong $\delta-$like peaks at low magnetic fields.

Finalizing our description of the impact of the electrostatic modulation on the Hofstadter spectrum, we would like to comment on how the standard Dirac cone type of energy dispersion would be modified in the presence of

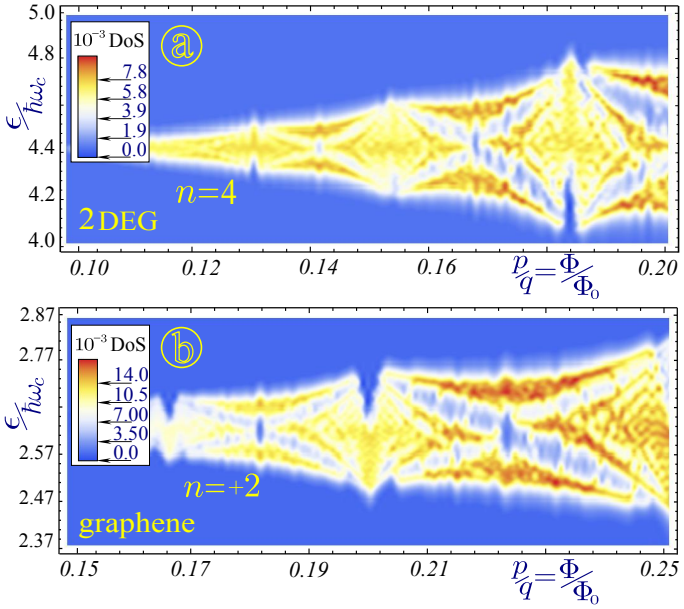

FIG. 5: (Color online) (Color online) Density-of-states plots for modulated 2DEG and graphene. Panel (a) shows the density of states for a 2DEG with modulation $\mathbb{V}_0 = 0.5\,\hbar\omega_c$ and modulation parameter $N = 5$. Plot (b) demonstrates the corresponding situation for graphene with $\mathbb{V}_0 = 1.5\,\hbar\omega_c$ and $N = 3$. For both plots (a) and (b), the density-of-states amplitude is increased proportionally to the value of magnetic field in order to make the Hofstadter structure visible at large fields.

modulation only, without the magnetic field. This situation could be described by the following Hamiltonian: $\mathcal{H}_{\mathbb{V}} = \sigma \cdot \mathbf{p} + \mathbb{V}(x,y)\mathcal{I}$ with $\mathbb{V}(x,y)$ given in Eq.(1) and $\mathcal{I}$ is the unit matrix. Obviously, we are dealing with the continuous spectrum, accompanied generally by a strong anisotropic dependence on k_x and k_y wave numbers. The wave function, corresponding to such periodic potential also satisfied the Bloch condition (4). Such a Hamiltonian with a periodic potential in one dimension was considered in [33]. Their results show that new zero energy states emerge and the wave function corresponds to an overdamped particle in a periodic potential. These zero energy solutions in fact represent new Dirac points. The presence of the zero-averaged wavenumber gaps as well as extra Dirac points in the band structure for the graphene-based one-dimensional superlattices were also found in [34]. The effect of non-homogeneous magnetic and electric fields was addressed in [35].

In summary, the well established Dirac fermion model is utilized to investigate the Landau level spectra of monolayer graphene in the presence of a periodic electrostatic potential. The intrinsic pseudospins from different Landau orbits which mix effectively give rise to multiple splitting of Landau levels. By incorporating Bloch wave function characteristics, we established an eigenvalue equation which yields fractal self-similar structure for the allowed energy band structure determined by the orbital pseudo spin and magnetic field signatures. In our calculations for the density-of-states, the physical origins of self-similarity are clearly established as being accessible experimentally. In particular, the emergence of Hofstadter's butterfly spectrum lies within a reasonable range of magnetic field that is currently available. Our numerical results clearly demonstrate magnetic field control of the energy density locations of the charge carriers and provide a basis for future experiments where regions of high absorption and conductivity may be observed at certain field strength. On the contrary, in the absence of magnetic field, the density-of-state lines are aligned next to each other.

This research was supported by contract # FA 9453-13-1-0291 of AFRL.

[1] B. Hunt et al., Science, **340**, 1427 (2013).
[2] R. Dean, et al., Nature **497**, 598 (2013).
[3] L. A. Ponomarenko, et al. Nature **497**, 594 (2013).
[4] M. Ya. Azbel, Sov. Phys. JETP, **19**, 634 (1964).
[5] D. R. Hofstadter, Phys. Rev.B **14**, 2239 (1976).
[6] Jung, J., DaSilva, A., Adam, S. and MacDonald, A. H., arXiv:**1403.0496** (2014).

[7] Woods, C. R., et al., arXiv:**1401.2637** (2014).
[8] Janecek, S. and Aichinger, M. and Hernández, E. R., Phys. Rev. B, **87**, 235429 (2013).
[9] Andrew L. C. Hayward, Andrew M. Martin and Andrew D. Greentree, PRL **108**, 223602 (2012).
[10] Godfrey Gumbs and Paula Fekete, Phys. Rev. B **56**, 3787 (1997).
[11] G. H. Wannier, Phys. Stat. Sol. **b100**, 163 (1980).
[12] A. Rauh, G. H. Wannier, and G. Obermair, Phys. Stat. Solidi b **63**, 215 (1974).
[13] A. Rauh, Phys. Stat. Sol. **b69**, K9 (1975).
[14] H. W. Neumann and A. Rauh, Phys. Stat. Solidi b **96**, 233 (1979).
[15] Y. Hasegawa, Y. Hatsugai, M. Kohmoto, and G. Montambaux, Phys. Rev. B **41**, 9174 (1990).
[16] Y. Hatsugai and M. Kohmoto, Phys. Rev. B **42**, 8282 (1990).
[17] D. Pfannkuche and R. R. Gerhardts, Phys. Rev. B **46**, 12606 (1992).
[18] D. Pfannkuche and R. R. Gerhardts, Surf. Sci. **263**, 324 (1992).
[19] D. J. Thouless, Phys. Rev. B **28**, 4272 (1983).
[20] F. Claro, Phys. Stat. Sol. (b) **104**, K31 (1981).
[21] H. J. Schellnhuber and G. M. Obermair, Phys. Rev. Lett. **45**, 276 (1980).
[22] T. Perschel and T. Geisel. Phys. Rev. Lett. **71**, 239 (1993).
[23] X. Wu and S. E. Ulloa, Phys. Rev. B **47**, 10028 (1993).
[24] H. Silbernauer, J. Phys.: Condens. Matter **4**, 7355 (1992).
[25] J, B. Sokoloff, Physics Reports **126**, 189 (1985).
[26] O. Kühn, V. Fessatidis, H. L. Cui, P. E. Selbmann, and N.Horing, Phys. Rev.B **47**, 19, 13019 (1993).
[27] N. Nemec and G. Cunibert, Phys.Rev.B **75**, 201404(R) (2007).
[28] S. Drscher, P. Roulleau, F. Molitor, P. Studerus, C. Stampfer, K. Ensslin, and T. Ihn, Appl. Phys. Lett. 96, 152104 (2010).
[29] P. D. Ye, D. Weiss, R. R. Gerhardts, M. Seeger, K. von Klitzing, K. Eberl, and H. Nickel, Phys. Rev. Lett. **74**, 3013 (1995).
[30] M. Zarenia, P. Vasilopoulos, and F. M. Peeters, Phys.Rev. B, **85**, 245426 (2012).
[31] Gumbs, G., Iurov, A., Huang, D., Fekete, P., and Zhemchuzhna, L., arXiv:**1309.6953** (2013).
[32] Nemec, Norbert and Cuniberti, Gianaurelio, Phys. Rev. B, **74**, 165411 (2006).
[33] Brey, L. and Fertig, H. A., Phys. Rev. Lett., **103** 046809 (2009).
[34] Wang, Li-Gang and Zhu, Shi-Yao, Phys. Rev. B, **20** 205444 (2010)
[35] Tan, Liang Zheng and Park, Cheol-Hwan and Louie, Steven G., Phys. Rev. B, **81**, 195426 (2010).